Supplement of Atmos. Chem. Phys., 22, 12727–12748, 2022
https://doi.org/10.5194/acp-22-12727-2022-supplement

Atmospheric Chemistry and Physics
Open Access

Supplement of

Modeling coarse and giant desert dust particles

Eleni Drakaki et al.

Correspondence to: Eleni Drakaki (eldrakaki@noa.gr)

Supplement

Figure S1 shows a comparison between the drag coefficients given by Stokes Clift and Gauvin, (1971) along with its relevant difference with respect to the Reynolds number Re. The comparison shows that the drag coefficient by Clift and Gauvin, (1971) can be 2 times higher than Stoke's drag coefficient, for Re up to 1, suggesting the necessity of the implementation of the revised drag coefficient.

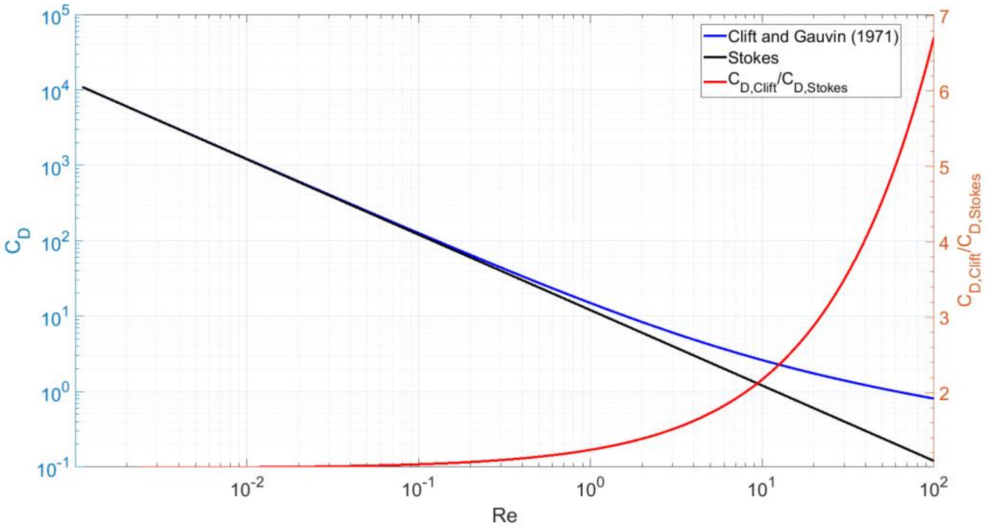

Figure S1: Drag coefficient for spheres given by the Stoke's approximation (black line) and the expression proposed by Clift and Gauvin (1971) (blue line). In the red line is the relative difference between the two drag coefficients.

It is quite difficult to quantify exactly the differences in the shape of PSD between 1 km and near surface PSDs. This is the reason why we choose to rely on the measured FENNEC-PSD at 1 km neglecting the sedimentation from this altitude down to the surface. However, in order to assess a possible impact of a PSD with greater contribution of coarse and large particles in the model ability to transport them, we calculate a settling rate from the volume difference with height (dV/dz), derived from the observed FENNEC -PSDs of freshly uplifted dust at height 1 and 1.5 km (Figure S2a from Ryder et al., (2013)). Given that settling rate, we estimate with extrapolation, a new volume size distribution, which corresponds to the surface (blue solid line, Fig. S2a). The blue dashed line corresponds to the lognormal size distribution fitted to the blue solid line, hereafter FENNEC-PSD-0km. Then, we calculate the new $k_{factors}$ based on the volume size distribution FENNEC-PSD-0km. A comparison between the previously used $k_{factors}$ (based on FENNEC-PSD, black line) and the new ones (based on (FENNEC-PSD-0km, blue line) is shown below in the Fig. S2b, and it is evident that the contribution on bin 5 is greater than the FENNEC-PSD (at 1km) which is used in the paper. We used the new $k_{factors}$ to run an additional simulation CONTROL-nPSD. A comparison of the volume size distribution above an emission grid point (similar to Fig. 5 in the manuscript) from CONTROL (blue line) and CONTROL-nPSD (orange line) runs is presented in Fig. S3. According to the results, we notice only a small improvement using the FENNEC-PSD-0km. Despite the small improvement, the results suggest that the use of a coarser PSD have the tendency to improve the model PSD representation. A possible new set of measurements from near the sources, which reveal coarser PSDs near the ground, could be used in future studies.

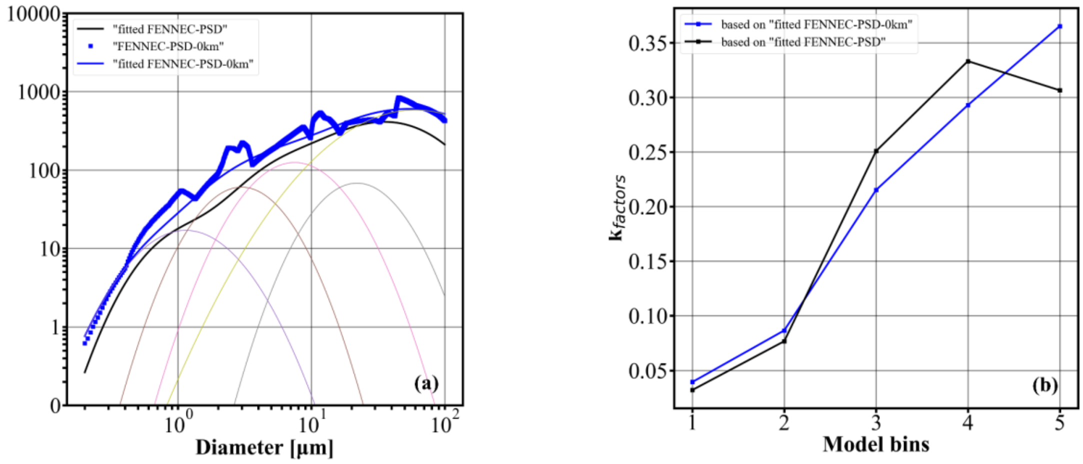

Figure S2: a) “fitted FENNEC-PSD” (black line), FENNEC-PSD-0km (blue squares) estimated with extrapolation applying the same volume difference per meter as that which holds between the measurements at 1km and 1.5km , and the corresponding “fitted FENNEC-PSD-0km” (blue solid line).

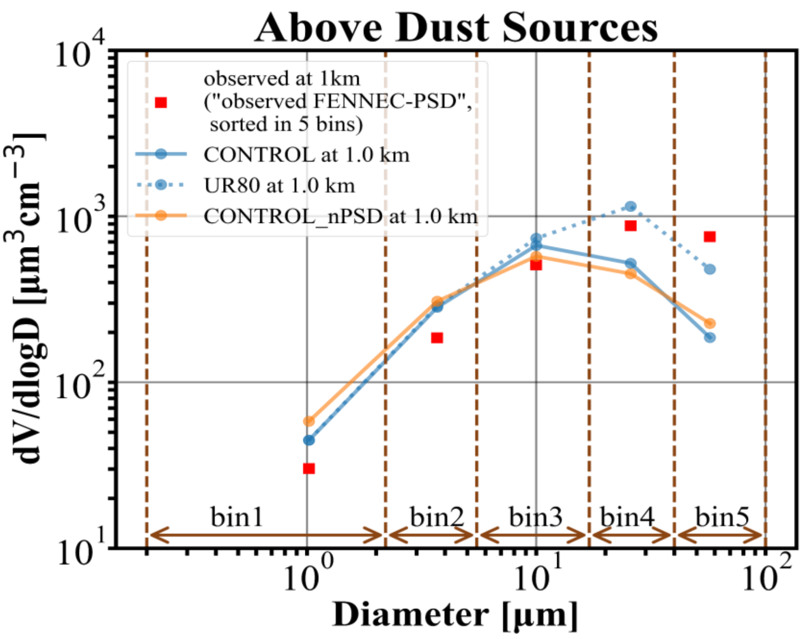

Figure S3: the observed averaged over 500 m, volume size distribution of freshly uplifted dust during FENNEC 2011 campaign (red squares), the model volume size distribution above a source grid point from CONTROL run (blue line) and from CONTROL-nPSD (orange line).

Figure. S4 shows the comparison (similar to Fig. 7) of the modelled and observed PSD in the downwind area, above the Atlantic Ocean during AER-D campaign.

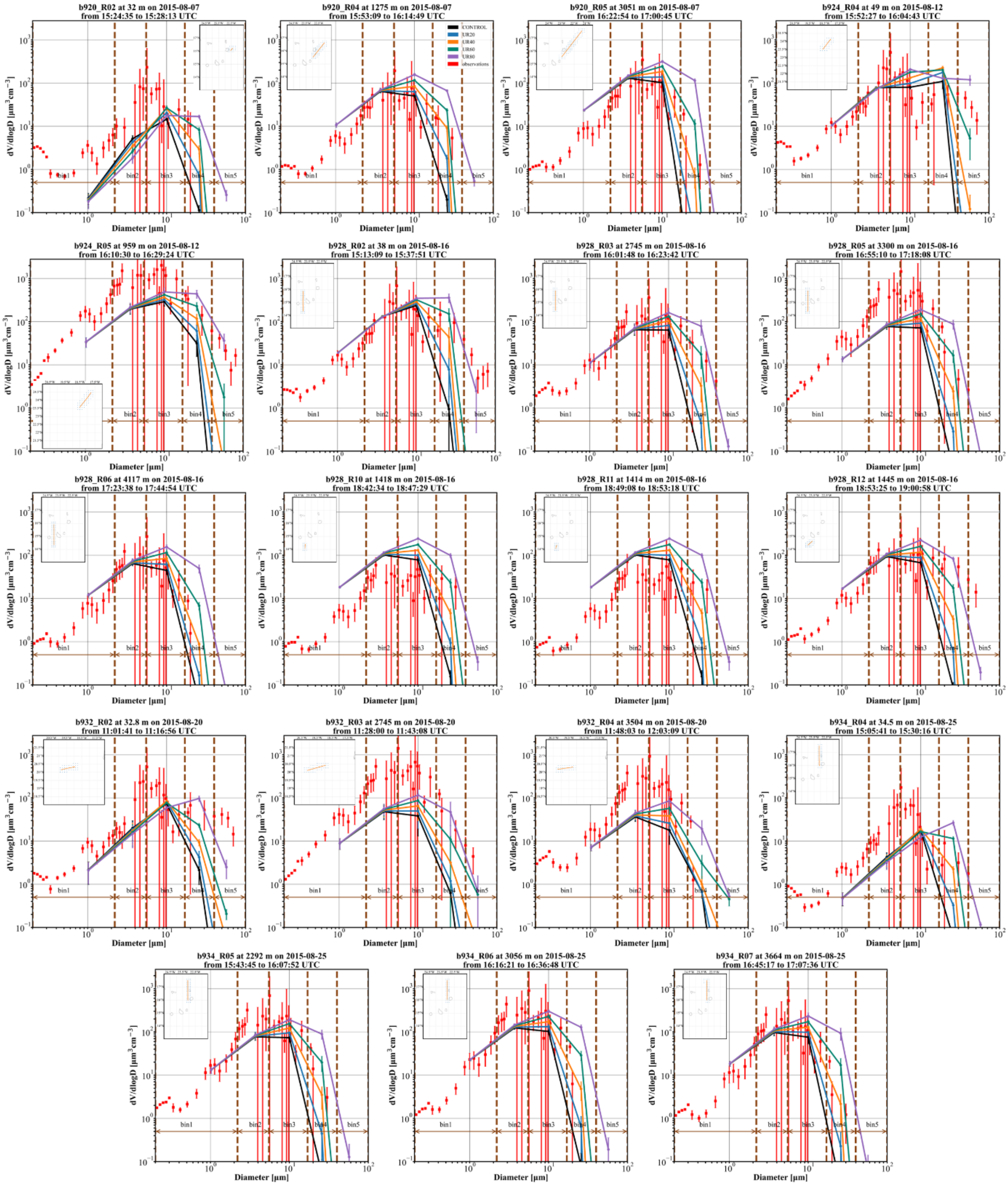

Figure S4: Modelled and observed dust PSD of flights RUNS, b920 R02, b920 R04, b920 R05, b924 R04, b924 R05, b928 R02, b928 R03, b928 R05, b928 R06, b928 R10, b928 R11, b928 R12, b932 R02, b932 R03, b932 R04, b934 R04, b934 R05, b934 R06 and b934 R07. The in situ observations are shown with red squares (along with the total instrumentation error). The collocated modelled PSDs are shown with lines, for the CONTROL run (black), UR20 (blue), UR40 (orange), UR60 (green), and UR80 (purple) and the corresponding standard deviation with the associated error bars. The brown vertical lines indicate the limits of the model size bins. The inlet maps show the flight segment track and the collocated model grid points.

Figure S5 shows a comparison of the different scenarios included in the two studies (Table S1). The corresponding calculations have been performed assuming US Standard

Atmosphere conditions. A reduction of particle density reduced by a factor of 10 (starting from the Clift and Gauvin, (1971) drag coefficients) is almost equivalent to a decrease of 90% in the settling velocities.

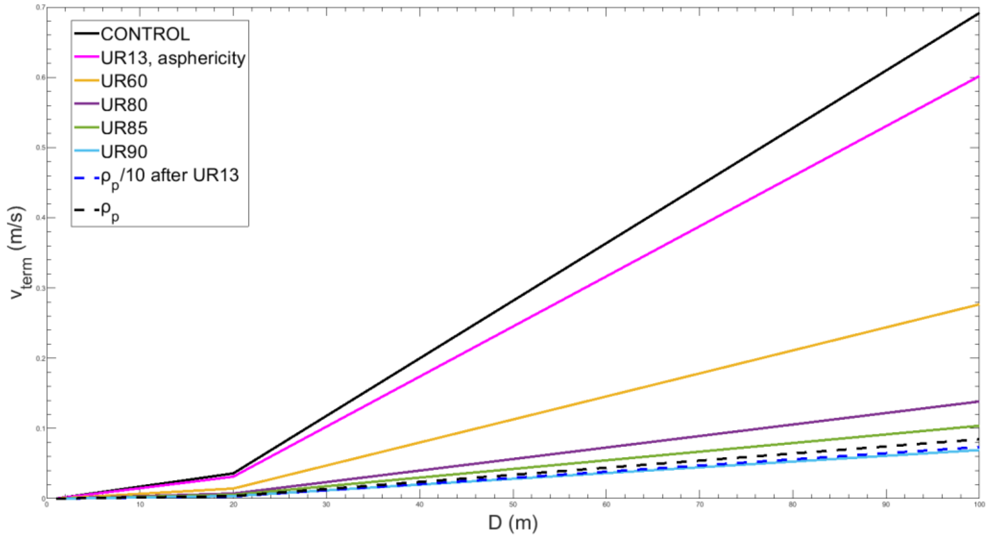

Figure S5: Terminal settling velocities with respect to particle diameter for dust particles, starting from the drag coefficient of Clift and Gauvin, (1971) and for the different scenarios described in Table S1.

Table S1: Different numerical experiments presented in Fig. S5

Cases	Description
UR60	**settling velocity reduced by 60%**
UR80	**settling velocity reduced by 80%**
UR13	**settling velocity reduced by 13%**
$\boldsymbol{\frac{\rho_D}{10}}$	**particle densities reduced by a factor of 10**
UR13&$\boldsymbol{\frac{\rho_D}{10}}$	**particle densities reduced by a factor of 10 and settling velocity reduced by 13%**
UR85	**settling velocity reduced by 85%**
UR90	**settling velocity reduced by 90%**

References

Clift, R. and Gauvin, W. H.: Motion of entrained particles in gas streams, Can. J. Chem. Eng., 49(4), 439–448, doi:10.1002/cjce.5450490403, 1971.

Huang, Y., Adebiyi, A. A., Formenti, P. and Kok, J. F.: Linking the Different Diameter Types of Aspherical Desert Dust Indicates That Models Underestimate Coarse Dust Emission, Geophys. Res. Lett., 48(6), doi:10.1029/2020GL092054, 2021.

Meng, J., Huang, Y., Leung, D. M., Li, L., Adebiyi, A. A., Ryder, C. L., Mahowald, N. M. and Kok, J. F.: Improved Parameterization for the Size Distribution of Emitted Dust Aerosols Reduces Model Underestimation of Super Coarse Dust, Geophys. Res. Lett., 49(8), e2021GL097287, doi:https://doi.org/10.1029/2021GL097287, 2022.

Ryder, C. L., Highwood, E. J., Lai, T. M., Sodemann, H. and Marsham, J. H.: Impact of atmospheric transport on the evolution of microphysical and optical properties of Saharan dust, Geophys. Res. Lett., 40(10), 2433–2438, doi:10.1002/grl.50482, 2013.